The Journal of Veterinary Medical Science

NOTE

Pathology

Canine adrenocorticotropic hormone-producing sinusoidal neuroendocrine tumor associated with Cushing's disease

Yeong-Bin BAEK[1)#], Mary Jasmin ANG[1)#], Jun-Gyu PARK[1)], DoHyeon YU[2)], Seungjo PARK[3)], Jae-Hyuk LEE[4)], Jihye CHOI[3)]* and Kyoung-Oh CHO[1)]*

[1)]Laboratory of Veterinary Pathology, College of Veterinary Medicine, Chonnam National University, Gwangju, 61186, Republic of Korea
[2)]Institute of Animal Medicine, College of Veterinary Medicine, Gyeongsang National University, Jinju, 52828, Republic of Korea
[3)]Veterinary Medical Imaging, College of Veterinary Medicine, Chonnam National University, Gwangju, 61186, Republic of Korea
[4)]Department of Pathology, Chonnam National University Medical School, Hwasun, 58128, Republic of Korea

J. Vet. Med. Sci.
81(12): 1863–1867, 2019
doi: 10.1292/jvms.19-0386

Received: 23 July 2019
Accepted: 15 October 2019
Advanced Epub:
28 October 2019

ABSTRACT. An 18-year-old male Yorkshire Terrier was admitted with a history of neurological signs including dullness and progressive tetraparesis. Physical examination revealed bilaterally symmetrical alopecia and pot-bellied abdomen. Computed tomography and necropsy examination showed a mass across the frontal sinus and cerebral frontal lobe, bilateral adrenocortical hyperplasia, and hepatomegaly. Histopathologically, the tumor lesions consisted of sheets, nests, or cords of small- to medium-sized round-to-polyhedral cells. Adrenal cortex showed bilateral diffuse cellular proliferation, and some hepatocytes showed intracytoplasmic glycogen accumulation. Immunohistochemically, the tumor cells were positive for pancytokeratin, chromogranin-A, neuron-specific enolase, S100, synaptophysin, and thyroid transcription factor-1 but negative for microtubule-associated proein-2 and neurofilament, leading to the diagnosis of neuroendocrine tumor. These tumor cells were also positive for adrenocorticotropic hormone.

KEY WORDS: adrenocorticotropic hormone, canine, Cushing's disease, neuroendocrine tumor

Neuroendocrine tumors (NETs) are rare tumors in domestic animals. In dogs and cats, these tumors occur in the intestines, esophagus, lungs, naso-oral cavity and skin [13–16, 18, 23]. In humans, the most common sites are the gastrointestinal and respiratory tracts [2, 6, 10, 22]. Most of these tumors are malignant and aggressive [13, 18, 20, 23]. Identification of NETs primarily relies on histopathological, immunohistochemical, and ultrastructural findings [8, 9, 13–16, 19, 21]. As the clinical, histopathological, and immunohistological characteristics of these tumors, particularly in the nasal cavities and brain, are similar to other tumors, such as olfactory neuroblastomas, differential diagnosis is usually required [24]. NETs are rarely functional in animals to secrete hormones, including glucagon and serotonin, leading to hormone-associated diseases [1, 3, 17, 20]. As far as we known, adrenocorticotropic hormone (ACTH)-producing NET has been only reported in one dog [3]. The present report describes the computed tomographical, histopathological, and immunohistochemical findings of ACTH-producing NET found in the sinusoidal cavity and brain in an 18-year-old dog in association with Cushing's disease.

An 18-year-old, male, Yorkshire Terrier was admitted to the Chonnam National University Veterinary Teaching Hospital with a history of neurological signs including dullness and progressive tetraparesis for 3 months, and a perianal tumor. Physical examination revealed severe, bilaterally symmetric alopecia with pot-bellied distended abdomen. Blood test revealed stress leukogram such as neutrophilia (12.56 K/μl over the reference range, 2.95–11.64 K/μl), monocytosis (1.61 K/μl over the reference range, 0.16–1.12 K/μl) and eosinopenia (0.02 K/μl below the reference range, 0.06–1.23 K/μl) and elevated alkaline phosphatase (714 U/l over the reference range, 23–212 U/l). Enlargement of bilateral adrenal glands without change in shape was detected on ultrasonography. Further imaging via computed tomography (CT) showed multiple masses in the frontal sinus, brain, stomach wall, and testes. In the reformatted sagittal plane (Fig. 1A), the sinusoidal tumor destroyed the cribriform plate and frontal bone,

*Correspondence to: Choi, J.: imsono@jnu.ac.kr, Cho, K.-O.: choko@jnu.ac.kr
#These authors contributed equally to this work.

©2019 The Japanese Society of Veterinary Science

This is an open-access article distributed under the terms of the Creative Commons Attribution Non-Commercial No Derivatives (by-nc-nd) License. (CC-BY-NC-ND 4.0: https://creativecommons.org/licenses/by-nc-nd/4.0/)

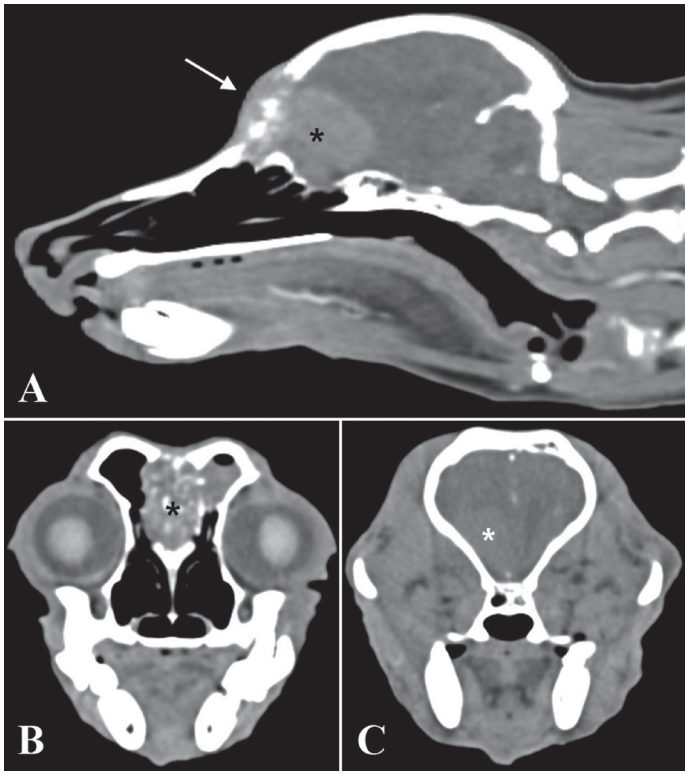

Fig. 1. Head, dog, computed tomography. (A) Reformatted sagittal image of the head shows a mass in the cerebral frontal lobe (asterisk) invading the subcutaneous tissue through the frontal bone (arrow). (B) A transverse image of the sinonasal region reveals a hyperattenuated mass (asterisk) in the left frontal sinus. (C) A well-outlined mass in the cerebral frontal lobe (asterisk).

invading into the left cerebral frontal lobe and forming a hyperattenuated mass (1.5 × 2 × 3 cm). Serial transverse images of the sinonasal region showed a hyperattenuated mass, measuring 1.5 × 2 × 3 cm, in the left frontal sinus (Fig. 1B) and left cerebral frontal lobe (Fig. 1C). The mass showed strong homogeneous contrast enhancement on post-contrast imaging. Midline shift and displacement of the left ventricle to the right side were observed. There was no abnormal finding of the pituitary gland in size, shape, and density on the pre- and post-contrast CT images.

The animal finally fell into a coma and was euthanized to relieve from this terminal illness by intravenous injection of potassium chloride after anesthesia by an intramuscular injection of a combination of 1.5 mg/kg zolazepam hydrochloride-tiletamine hydrochloride (Zoletil, Virbac, Carros, France) and 0.03 mg/kg medetomidine (Domitor, Oriion Corp., Espoo, Finland). Grossly, in consistent with the CT results, a white-to-greyish tumor mass was observed in the left cerebral frontal lobe over the cribriform plate starting from the left frontal sinus (Fig. 2A). The left testis contained a sharply delineated, soft, bulging yellow mass of 2.4 × 2 cm in diameter. The adrenal glands showed severe diffuse bilateral cortical hyperplasia, resulting in an increased cortico-medullary ratio of 3:1. Gross abnormality in the pituitary gland was not observed.

For histopathological examination, the tumor masses and major organs were fixed in 10% neutral buffered formalin, embedded in paraffin-wax, sectioned (3 μm), and routinely stained with hematoxylin and eosin (H&E). The selected sections were also subjected to immunohistochemistry (IHC) and Grimelius stain. To identify the nature of swollen hepatocytes, formalin-fixed, frozen liver sections were stained with Periodic acid-Schiff (PAS) reaction. Microscopically, the tumor masses in the left frontal sinus and left cerebral frontal lobe were composed of small-to-medium-sized cells arranged in nests separated by a delicate fibrovascular stroma in the sinus and a neuropil stroma, giving an endocrine-type packaging (Fig. 2B). The tumor cells were round to polyhedral, containing round-to-polyhedral nuclei with distinct nucleolus and a distinct granular eosinophilic cytoplasm (Fig. 2C). Large clear neoplastic cells were mixed with round-to-polyhedral cells in some tumor islands. The peripheral tumor cells in the tumor nests and islands showed a palisading appearance. Homer-Wright rosette formation was rarely found in the tumor lesions (Fig. 2D). Some tumor nests underwent central necrosis containing necrotic debris, macrophages, and neutrophils (Fig. 2B). By Grimelius stain, the tumor cells contained intracytoplasmic endocrine granules (Fig. 2E). The pituitary gland showed no abnormality. The adrenal cortex in both glands showed diffuse proliferation of cells, with alveolar and trabecular patterns. The liver had severe, multiple, locally extensive swollen hepatocytes, which were due to glycogen accumulation confirmed by PAS reaction (Fig. 2F). These findings suggested severe bilateral adrenocortical hyperplasia and resulting glucocorticoid-induced hepatopathy. In other organs, leiomyoma (stomach), Leydig cell tumor (testis) and hepatoid gland adenoma (perianal gland) were observed, respectively.

To differentiate the tumors in the frontal sinus and cerebral frontal lobe, IHC was performed with 3-μm-thick selected sections using the Dako REAL^{TM} EnVision^{TM} Detection System (DakoCytomation, Denmark), following the manufacturer's instructions. Tissue sections were incubated overnight in a moist chamber at 4°C with antibodies (Table 1). For negative control, the primary antibodies were replaced with phosphate-buffered saline (PBS, pH 7.4). Table 1 shows various immunolabelling reactivities of the tumor cells with various antibodies. The tumor cells were positive for pancytokeratin, chromogranin-A, neuron-specific enolase (NSE), S100,

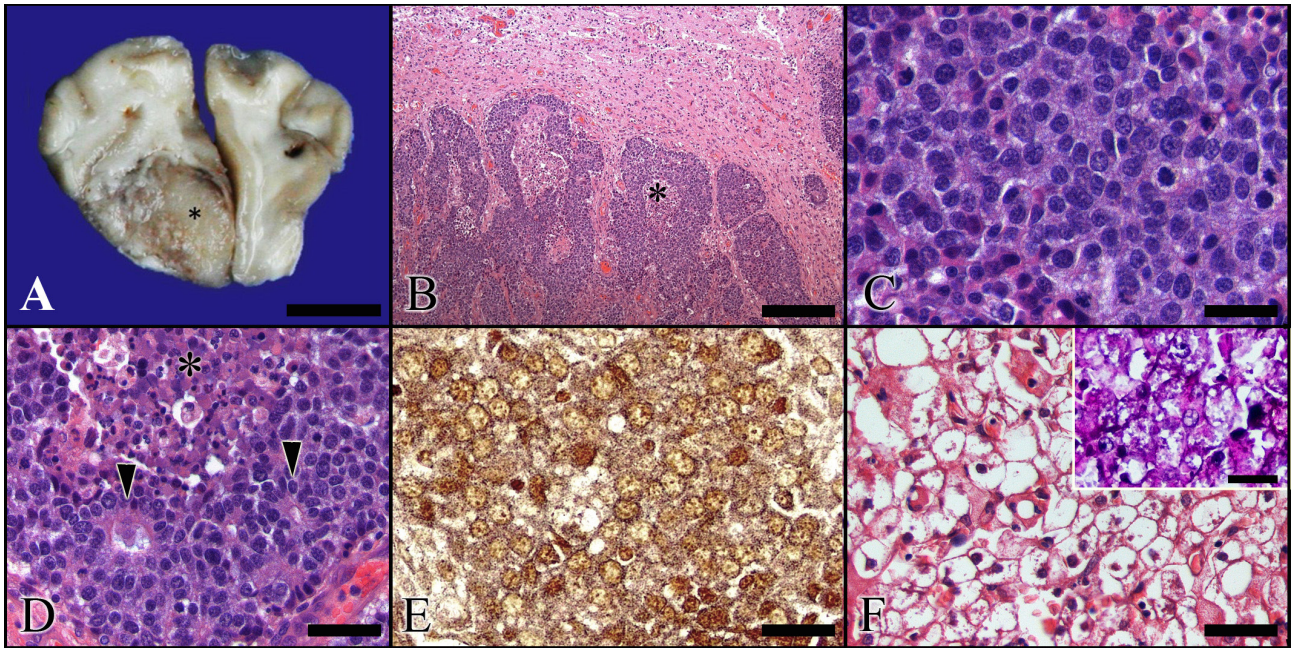

Fig. 2. Gross and histopathological findings. (A) A cross-section through the frontal lobe. The tumor (asterisk) occupies the lower right frontal lobe, compressing the left frontal lobe. Bar=1 cm. (B) The tumor mass consists of nests of small-to-medium-sized cells separated by a neuropil stroma; some tumor nests undergo central necrosis (asterisk), characterized by necrotic debris, macrophages, and neutrophils. H&E. Bar=200 μm. (C) Tumor cells are round to polyhedral, containing round-to-polyhedral, centrally located nuclei and distinct granular, hyperchromatic cytoplasm. H&E. Bar=30 μm. (D) Homer-Wright rosette formation characterized by central neurophil and peripheral tumor cells (arrow). The tumor nest has central necrosis (asterisk). H&E. Bar=40 μm. (E) Tumor cells contain many intracytoplasmic endocrine granules. Grimelius stain. Bar=25 μm. (F) The liver has severe, multiple, locally extensive swollen hepatocytes, which show intracytoplasmic glycogen accumulation identified by Periodic acid-Schiff reaction (inset). H&E and Periodic acid-Schiff reaction. Bars=40 μm.

Table 1. Primary antibodies used in immunohistochemistry

Antigen	Type	Dilution	Antigen retrieval	Source	Reactivity
Pancytokeratin	Mouse Mab	1:50	HIAR[a)]	DakoCytomation, Glostrup, Denmark	Positive
Chromogranin-A	Rabbit PCab	1:400	HIAR[a)]	Novus Biotech, Centennial, CO, U.S.A.	Positive
NSE	Mouse Mab	1:100	HIAR[a)]	Millipore, Burlington, MA, U.S.A.	Positive
S100	Rabbit PCab	1:400	HIAR[b)]	DakoCytomation, Glostrup, Denmark	Positive
Synaptophysin	Mouse Mab	1:400	HIAR[a)]	DakoCytomation, Glostrup, Denmark	Positive
CD56	Mouse Mab	1:200	HIAR[a)]	DakoCytomation, Glostrup, Denmark	Positive
TTF-1	Mouse Mab	1:200	HIAR[a)]	DakoCytomation, Glostrup, Denmark	Positive
ACTH	Mouse Mab	1:50	HIAR[a)]	Santa Cruz Biotech, Dallas, TX, U.S.A.	Positive
MAP2	Mouse Mab	1:500	HIAR[c)]	Sigma-aldrich, St. Louis, MO, U.S.A.	Negative
Neurofilament	Mouse Mab	1:400	HIAR[a)]	Sigma-aldrich, St. Louis, MO, U.S.A.	Negative
CNPase	Mouse Mab	1:100	HIAR[c)]	Merck, Darmstadt, Germany	Negative
GFAP	Rabbit PCab	1:1,000	HIAR[c)]	DakoCytomation, Glostrup, Denmark	Negative
CDX-2	Mouse Mab	1:50	HIAR[a)]	DakoCytomation, Glostrup, Denmark	Negative

NSE, neuron-specific enolase; TTF-1, thyroid transcription factor 1; ACTH, adrenocorticotropic hormone; MAP2, microtubule-associated protein 2; CNPase, 2′,3′-cyclic nucleotide-3′-phosphodiesterase; GFAP, glial fibrillary acidic protein; Mab, mouse monoclonal antibody; PCab, rabbit polyclonal antibody; HIAR, heat-induced antigen retrieval (a) microwave: 100°C/10 mM Tris buffer for 20 min; b) microwave: 100°C/10 mM citrate buffer for 20 min; c) autoclaving at 121°C in 10 mM citrate buffer for 10 min).

and synaptophysin, which are makers for NETs and olfactory neuroblastomas (Fig. 3A–E). However, tumor cells were negative for microtubule-associated protein 2 (MAP2) and neurofilament, as it could differentiate from olfactory neuroblastomas. In addition, tumor cells were negative for neuronal and glial cell markers (glial fibrillary acidic protein [GFAP], and 2′,3′-cyclic nucleotide-3′-phosphodiesterase [CNPase], ruling out astrocytoma, oligodendroglioma, ependymoma, and gangliocytoma. Antibody against CD56 antigen (also known as neural cell adhesion molecule), which is detected in human NETs as well as non-Hodgkin lymphoma-natural killer cell type and other hematological malignancies [4], identified some tumor cells in the present case (Fig. 3F). Antibody against thyroid transcription factor-1 (TTF-1), which is used for identifying human respiratory NETs [6, 10], labeled the tumor cells (Fig. 3G)

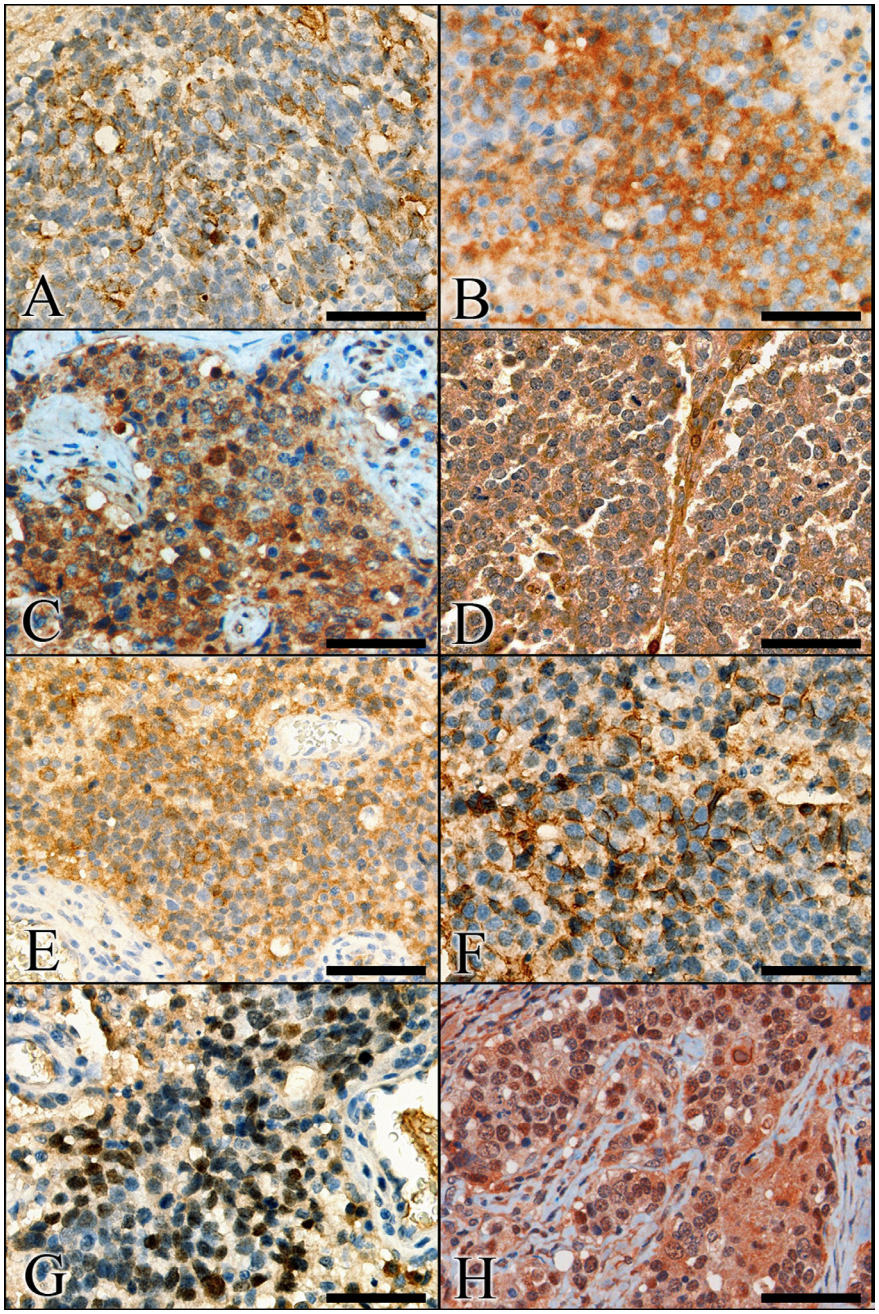

Fig. 3. Immunohistochemical findings. (A–N) The tumor cells are found to be positive for pancytokeratin (A), chromogranin-A (B), neuron-specific enolase (C), S100 (D), synaptophysin (E), CD56 (F), thyroid transcription factor-1 (G), and adrenocorticotropic hormone (H). Immunostaining with hematoxylin counter stain. Bars=50 μm.

by cross reactivity of this antibody to dog cells. The CDX-2 antibody, which is used for determining human intestinal NETs [6, 10], did not react in the tumor cells. Interestingly, antibody against ACTH detected the tumor cells (Fig. 3H).

The characteristic morphological and immunohistochemical findings suggested sinusoidal NET in the present case. However, NET and olfactory neuroblastomas have some common histopathological and immunohistochemical characteristics, such as microscopic rosette formation and positive immunoreactivity for some neural and neuroendocrine markers (NSE, synaptophysin, S100, and chromogranin-A), making it difficult to distinguish these tumors [24]. Some neuronal tumor makers including MAP2, neurofilament, and class III beta-tubulin isotype can differentiate these tumors, all of which are positive for neuroblastomas but negative for NETs [9, 20, 24]. The tumor cells in the present case were negative for MAP2 and neurofilament, which can differentiate this tumor from olfactory neuroblastomas. In addition, negative IHC reactions of this tumor with MAP2, GFAP, CNPase, and Iba1 allowed differentiation from neurogenic tumors, such as astrocytoma, oligodendroglioma, ependymoma, and gangliocytoma [7].

In animals, hematogenous dissemination plays a major role in tumor metastasis to the central nervous system, while the remainder is caused by local direct invasion [7]. Secondary intracranial tumors with hematogenous origin were usually multiple, well-circumscribed, round masses. In veterinary literature, direct invasion of nasal NETs have rarely been reported [5, 7]. In the present case, NET was found across the frontal sinus and cerebral frontal lobe. Moreover, NETs were not found in other organs or tissues on CT or gross or histopathological examination, indicating that the tumor was not metastasized from any other organ.

Therefore, invasion of the frontal sinusoidal NET through the cribriform plate in the olfactory bulbs and frontal lobes is plausible [7]. As primary NETs in the brain have been reported in humans [11, 12, 22], direct invasion of the olfactory bulb or frontal lobe by NETs through the cribriform plate into the frontal sinus could not be ruled out. In human pathology, TTF-1 and CDX-2 are used for the differentiation between pulmonary and intestinal NETs [10]. In the present study, tumor cells in the frontal sinus and brain were positive for TTF-1 but not for CDX-2, suggesting nasal origin of this tumor. To confirm this hypothesis, more intensified studies using many pulmonary, sinonasal, and intestinal NETs of dogs are needed.

Hormone hypersecretory syndromes caused by NETs have rarely been reported in animals compared to humans. For example, glucagonomas in the pancreas and liver can induce superficial necrolytic dermatitis through excessive glucagon production by tumor cells [1], whereas intestinal NETs can cause diarrhea through hypersecretion of serotonin [20]. In this case, physical examination revealed bilaterally symmetric alopecia and pot-bellied distended abdomen. Moreover, this case had bilateral adrenocortical hyperplasia and was suspected with glucocorticoid-induced hepatopathy. All these findings indicated that this case was of Cushing's disease. As there was no history of corticosteroid medication or gross or histopathological abnormality in the pituitary gland, Cushing's disease due to iatrogenic corticosteroid medication and functional pituitary gland tumor could be excluded [17]. Interestingly, tumor cells in the present case were positive for ACTH. This indicated that hypersecretion of ACTH from NET caused bilateral adrenocortical hyperplasia, and subsequently, excessive production of glucocorticoid hormone, which induced Cushing's syndrome.

REFERENCES

1. Allenspach, K., Arnold, P., Glaus, T., Hauser, B., Wolff, C., Eberle, C. and Komminoth, P. 2000. Glucagon-producing neuroendocrine tumour associated with hypoaminoacidaemia and skin lesions. *J. Small Anim. Pract.* **41**: 402–406. [Medline] [CrossRef]
2. Brehar, F. M., Gorgan, R. M. and Neacsu, A. 2013. Brain metastases of neuroendocrine tumor with unknown primary location−Case report. *Rom. Neurosurg.* **20**: 1–7.
3. Castillo, V. A., Pessina, P. P., Garcia, J. D., Hall, P., Gallelli, M. F., Miceli, D. D. and Blatter, M. F. C. 2014. Ectopic ACTH syndrome in a dog with a mesenteric neuroendocrine tumour: a case report. *Vet. Med.* **59**: 352–358. [CrossRef]
4. Farinola, M. A., Weir, E. G. and Ali, S. Z. 2003. CD56 expression of neuroendocrine neoplasms on immunophenotyping by flow cytometry: a novel diagnostic approach to fine-needle aspiration biopsy. *Cancer* **99**: 240–246. [Medline] [CrossRef]
5. Foster, E. S., Carrillo, J. M. and Patnaik, A. K. 1988. Clinical signs of tumors affecting the rostral cerebrum in 43 dogs. *J. Vet. Intern. Med.* **2**: 71–74. [Medline] [CrossRef]
6. Hang, J. F., Hsu, C. Y., Lin, S. C., Wu, C. C., Lee, H. J. and Ho, D. M. T. 2017. Thyroid transcription factor-1 distinguishes subependymal giant cell astrocytoma from its mimics and supports its cell origin from the progenitor cells in the medial ganglionic eminence. *Mod. Pathol.* **30**: 318–328. [Medline] [CrossRef]
7. Higgins, R. J., Bollen, A. W., Dickinson, P. J. and Sisó-Llonch, S. 2017. Tumors of the nervous system. pp. 834–891. *In*: Tumors in Domestic Animals, 5th ed. (Meutens, D. J. eds.), John Wiley & Sons Inc., Ames.
8. Johnson, G. C., Coates, J. R. and Wininger, F. 2014. Diagnostic immunohistochemistry of canine and feline intracalvarial tumors in the age of brain biopsies. *Vet. Pathol.* **51**: 146–160. [Medline] [CrossRef]
9. Kubo, M., Matsuo, Y., Okano, T., Sakai, H., Masegi, T., Asano, M., Uchida, K. and Yanai, T. 2009. Nasal neuroendocrine carcinoma in a free-living Japanese raccoon dog (Nyctereutes procyonoides viverrinus). *J. Comp. Pathol.* **140**: 67–71. [Medline] [CrossRef]
10. Lin, X., Saad, R. S., Luckasevic, T. M., Silverman, J. F. and Liu, Y. 2007. Diagnostic value of CDX-2 and TTF-1 expressions in separating metastatic neuroendocrine neoplasms of unknown origin. *Appl. Immunohistochem. Mol. Morphol.* **15**: 407–414. [Medline] [CrossRef]
11. Liu, H., Wang, H., Qi, X. and Yu, C. 2016. Primary intracranial neuroendocrine tumor: two case reports. *World J. Surg. Oncol.* **14**: 138. [Medline] [CrossRef]
12. Liu, H., Zhang, M., Wang, X., Qu, Y., Zhang, H. and Yu, C. 2016. Primary intracranial neuroendocrine tumor with ectopic adrenocorticotropic hormone syndrome: A rare and complicated case report and literature review. *Mol. Clin. Oncol.* **5**: 99–102. [Medline] [CrossRef]
13. Patnaik, A. K. 1992. A morphologic and immunocytochemical study of hepatic neoplasms in cats. *Vet. Pathol.* **29**: 405–415. [Medline] [CrossRef]
14. Patnaik, A. K., Erlandson, R. A. and Lieberman, P. H. 1990. Esophageal neuroendocrine carcinoma in a cat. *Vet. Pathol.* **27**: 128–130. [Medline] [CrossRef]
15. Patnaik, A. K., Ludwig, L. L. and Erlandson, R. A. 2002. Neuroendocrine carcinoma of the nasopharynx in a dog. *Vet. Pathol.* **39**: 496–500. [Medline] [CrossRef]
16. Patnaik, A. K., Newman, S. J., Scase, T., Erlandson, R. A., Antonescu, C., Craft, D. and Bergman, P. J. 2005. Canine hepatic neuroendocrine carcinoma: an immunohistochemical and electron microscopic study. *Vet. Pathol.* **42**: 140–146. [Medline] [CrossRef]
17. Rosol, T. J. and Meuten, D. J. 2017. Tumors of the endocrine glands. pp. 766–833. *In*: Tumors in Domestic Animals, 5th ed. (Meutens, D. J. eds.), John Wiley & Sons Inc., Ames.
18. Rossi, G., Magi, G. E., Tarantino, C., Taccini, E., Mari, S., Pengo, G. and Renzoni, G. 2007. Tracheobronchial neuroendocrine carcinoma in a cat. *J. Comp. Pathol.* **137**: 165–168. [Medline] [CrossRef]
19. Ruiz, F. S., Alessi, A. C., Chagas, C. A., Pinto, G. A. and Vassallo, J. 2005. Immunohistochemistry in diagnostic veterinary pathology: a critical review. *J. Bras. Patol. Med. Lab.* **41**: 263–270. [CrossRef]
20. Sako, T., Shimoyama, Y., Akihara, Y., Ohmachi, T., Yamashita, K., Kadosawa, T., Nakade, T., Uchida, E., Okamoto, M., Hirayama, K. and Taniyama, H. 2005. Neuroendocrine carcinoma in the nasal cavity of ten dogs. *J. Comp. Pathol.* **133**: 155–163. [Medline] [CrossRef]
21. Solcia, E., Kloppel, G., Sobin, L. H. and Williams, E. D. 2002. Histological typing of endocrine tumors. p. 2. *In*: World Health Organization. International histological Classification of Tumours, 2nd ed., Springer, Berlin.
22. Tamura, R., Kuroshima, Y. and Nakamura, Y. 2014. Primary neuroendocrine tumor in brain. *Case Rep. Neurol. Med.* **2014**: 295253. [Medline]
23. Whiteley, L. O. and Leininger, J. R. 1987. Neuroendocrine (Merkel) cell tumors of the canine oral cavity. *Vet. Pathol.* **24**: 570–572. [Medline] [CrossRef]
24. Wilson, D. W. 2017. Tumors of the respiratory tract. pp. 467–498. *In*: Tumors in Domestic Animals, 5th ed. (Meutens, D. J. ed.), John Wiley & Sons Inc., Ames.